CRYSTAL GROWTH & DESIGN

Article

pubs.acs.org/crystal

Structural Elucidation of the Neuraminidase Inhibitor Zanamivir (Relenza): Creeping and Diffusion for Polymorph Separation

Naba K. Nath,[†] Nobuhiro Yasuda,[‡] Wael M. Rabeh,[†] Subash Chandra Sahoo,[†] and Panče Naumov*[,†]

[†]New York University Abu Dhabi, POB 129188, Abu Dhabi, United Arab Emirates

[‡]Japan Synchrotron Radiation Research Institute, 1-1-1 Kouto, Sayo-cho, Sayo-gun, Hyogo 679-5198, Japan

Supporting Information

ABSTRACT: Zanamivir, the active ingredient of the antiviral drug Relenza, is the most potent of the four currently approved neuraminidase inhibitors for treatment of pandemic strains of influenza. A combination of solution creeping and vapor diffusion of antisolvent was successfully applied to obtain two crystalline polymorphic dihydrates and to accomplish the first structure determination of zanamivir with X-ray diffraction.

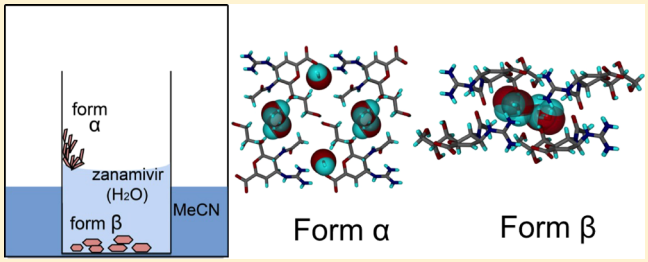

Since the 16th century, humanity has experienced 22 pandemics of influenza, with the "swine flu" (H1N1) pandemic outbreak in 2009 being the most recent pandemic.[1−3] The first commercial neuraminidase inhibitor is the antiviral drug zanamivir, marketed in the U.S. in 1999/2000 by GlaxoSmithKline (GSK) as "Relenza".[4] Together with oseltamivir (Tamiflu), introduced to the market by Roche as phosphate salt several months later, it is one of only four medicines that are currently approved for treatment of influenza.[5−7] Zanamivir[8,9] blocks the release of the influenza virus from the surface of the host cell by inhibiting the viral neuraminidase that catalyzes cleavage of terminal sialic acid residues attached to glycoproteins and glycolipids.[6,10] Chemically, zanamivir and oseltamivir are based on a single substituted hexacyclic moiety designed by computer-aided modeling to mimic the oxocarbonium ion intermediate (Scheme 1).

Scheme 1. Chemical Structures of Oseltamivir and Zanamivir in Their Neutral Forms, and the Key (Oxocarbonium) Intermediate That They Mimic in the Course of Neuraminidase Inhibition[a]

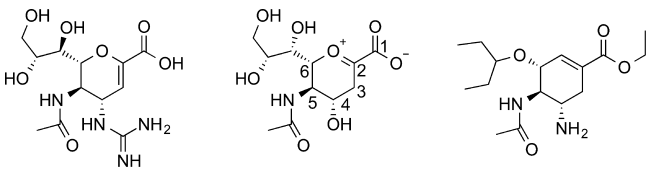

[a]The atom labeling convention follows that commonly used for sialic acid.

Although both zanamivir and oseltamivir bear the central cyclohexane moiety, only the former has the actual oxa(cyclohexene) ring of the oxo(carbonium) intermediate, with the double bond at position 2,3 instead of 2,7. A comparative study by the Centers for Disease Control and Prevention (CDC) of the efficacy of zanamivir and oseltamivir is in strong favor of the former for treatment of influenza; whereas 0.5% of the 2009 pandemic flu and as many as 99.6% of the tested viral strains of seasonal H1N1 flu were resistant to Tamiflu,[11−14] zanamivir was effective toward all seasonal and pandemic strains.

On the other hand, dosing of zanamivir is currently limited to the inhaled route in the form of a 1:4 mixture with lactose, which places burdens and restricts its usage with asthmatics. Only 4−17% of the inhaled dose is systemically absorbed, limiting the bioavailability of zanamivir to only 2%. Despite its higher antiviral potency, the reported cases of bronchospasm and respiratory failure with patients with respiratory diseases have restricted its use, and in 2009, zanamivir was outsold 1:3 billion U.S. dollars by Tamiflu, the latter being available as an oral tablet formulation. To overcome these issues, intravenous delivery of zanamivir[15−19] is under clinical trials.

The resistance of the H5N1 neuraminidase to oseltamivir indicates favorable binding of zanamivir relative to oseltamivir.[20] Information on the intermolecular interactions of zanamivir based on its supramolecular structure could shed light on its binding preferences and strong biological activity. However, because of problems with crystallization, its crystal structure has not been reported yet. Here, following our recent work on Tamiflu,[21] we report the crystal structure of zanamivir in hopes of providing an alternative explanation for the enhanced physiological activity of zanamivir relative to oseltamivir. During the crystallization trials of zanamivir, the diffusion of acetonitrile vapors as antisolvent in saturated solutions of zanamivir alleviated the solubility and facilitated crystallization. Simultaneously, the solution "creeped" along the glass walls of the container, and crystalline

Received: November 2, 2013
Revised: December 2, 2013
Published: December 9, 2013

   dx.doi.org/10.1021/cg4016383 | *Cryst. Growth Des.* 2014, 14, 770−774

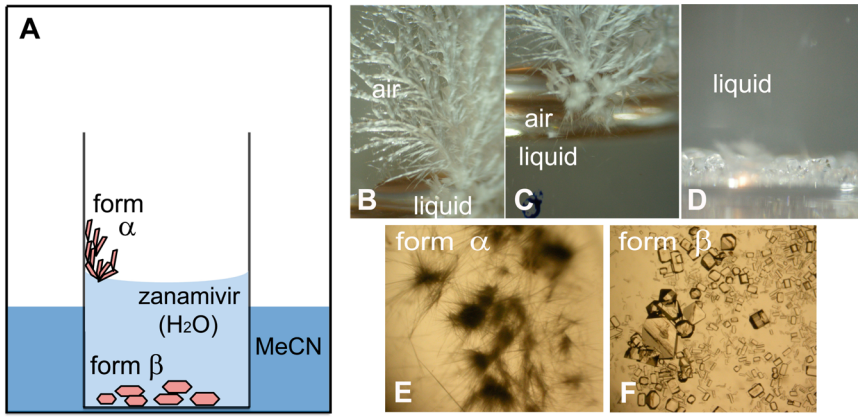

Figure 1. Crystals of the two polymorphic dihydrates, α (E) and β (F), of zanamivir, and snapshots of the crystallization process during diffusion of acetonitrile into saturated aqueous solution (B–D). Crystals of form α appear first on the walls of the container, and the crystallization continues from the solution that creeps up the walls. Crystals of form β appear at the bottom of the crystallization vessel.

material accumulated above the liquid–air surface.[22] Two zanamivir dihydrate polymorphs crystallized from the same batch at different locations of the container and were easily mechanically separated. To explain the unusual potency of zanamivir, we also compare the structures of the two zanamivir dihydrate polymorphs elucidated using synchrotron X-ray radiation with the structure of neuraminidase of the influenza virus.

Zanamivir dissolves well in water by vigorous stirring at room temperature. Both forms of zanamivir dihydrate crystallize by slow diffusion of acetonitrile vapors into the saturated aqueous solution at room temperature (Figure 1A). Upon exposure of the solution to acetonitrile in a closed glass vessel, bundles of colorless fine needle crystals or dendrimers (form α, Figure 1E) appear close to the liquid–air surface in about 1 day (Figure 1B). Due to the higher concentration of the antisolvent close to the surface of the solution, the crystals of form α grow close to the water–air surface, but mostly on the walls above the solution (Figure 1C). After 1 day, well-formed colorless blocky crystals of another form (form β, Figure 1F) appear exclusively at the bottom of the container (Figure 1D). The crystals of form β are stable in solution for months; they do not redissolve upon standing and can easily be separated by decantation. The two crystalline forms are readily distinguishable by their crystal habits (Figure 1E,F).

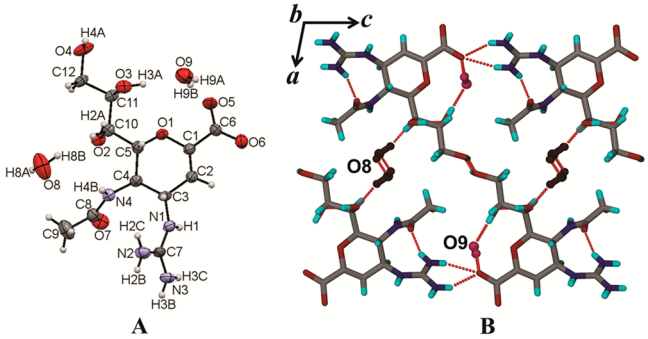

Figure 2. (A) ORTEP diagram of form α of zanamivir dihydrate. (B) Different molecular environments for the two symmetry-independent water molecules in the crystal lattice of form α. The two symmetry-independent molecules are shown in different colors. One of the water molecules (O8, brown) is in a channel forming helical chains and is hydrogen-bonded to the host, whereas the other water molecule (O9, pink) is isolated and forms a hydrogen bond to zanamivir.

The structures of the two polymorphs were determined from single crystals at 220 K (form α) and 223 K (form β) using synchrotron X-ray radiation (for details, see the Experimental Details section in the Supporting Information). In both structures, the zanamivir molecule exists as a zwitterion. The dihydropyran ring contains a number of hydrogen bond donors and acceptors: carboxylate (two acceptors), acetamido (one donor, one acceptor), guanidinium (five donors, three acceptors), and one primary and two secondary alcoholic O–H groups (each contains one donor and one acceptor). The two polymorphs show a pronounced dissimilarity, where the side groups of the zanamivir molecule have different conformations (Table S1 in the Supporting Information lists the torsion angles, and Figure S1 shows an overlapped diagram of two molecular conformations).

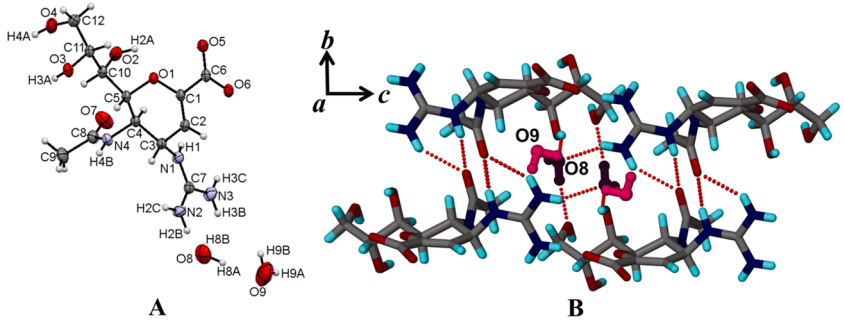

Figure 3. (A) ORTEP diagram of form β of zanamivir dihydrate. (B) The two symmetry-independent water molecules are situated in isolated sites with similar molecular environments and are hydrogen-bonded to the host.

dx.doi.org/10.1021/cg4016383 | Cryst. Growth Des. 2014, 14, 770–774

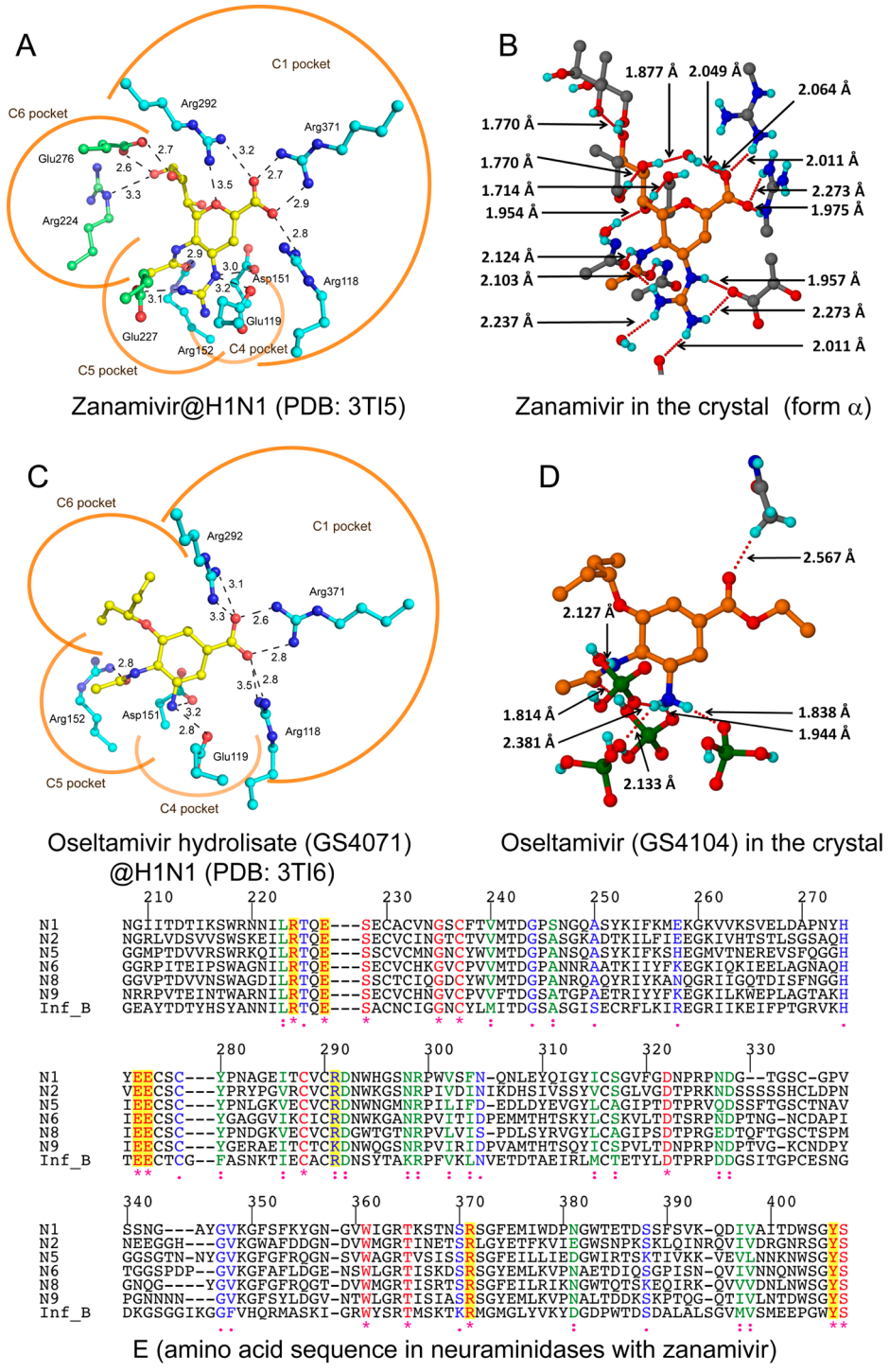

Figure 4. (A) Intermolecular interactions in the structure of H1N1, the 2009 pandemic neuraminidase (H1N1) in complex with zanamivir (PDB code: 3TI5). The carbons of the inhibitor are colored yellow. The NA's active site residues interacting with zanamivir only are colored green, and those interacting with zanamivir and oseltamivir are colored aqua. Nitrogen and oxygen atoms are colored blue and red, respectively. Glu277 and Tyr406 that interact with oxygen at position 1 of the zanamivir pyran ring are not shown for simplicity. The ionic interactions between zanamivir and C1 and C4 pockets of NA's active site offer tight binding interactions in comparison to the weaker hydrogen bond interactions with C5 and C6 pockets. (B) Interactions of zanamivir in the crystal of form *α*. (C) Intermolecular interactions in the structure of H1N1 in complex with oseltamivir (PDB code: 3TI6). Atoms are colored the same as in (A). The number of binding interactions between oseltamivir and NA's active site residues is less than those observed in the zanamivir complex. The illustration was generated using PyMOL Molecular Graphics System, Schrödinger, LLC. (D) Intermolecular interactions of oseltamivir in the pure crystal.[17]

Form *α* crystallizes as needles with $P2_1$ symmetry and contains one zanamivir zwitterion and two water molecules in the asymmetric unit. One of the symmetry-independent water molecules is situated in a channel to form 2_1 helical chains, while the other water molecule is in an isolated site forming a hydrogen bond (HB) to the host. The water molecules that form the helix are connected to each other and to the host via hydrogen bonds (HBs) O−H···O (O8−H8A···O8, $d_{H\cdots A}$ = 2.041 Å, $d_{D\cdots A}$ = 2.785 Å,

dx.doi.org/10.1021/cg4016383 | *Cryst. Growth Des.* 2014, 14, 770−774

$\theta_{D-H\cdots A}$ = 146.7°; O8−H8B···O2, 1.954 Å, 2.762 Å, 162.9°). The other symmetry-independent water molecules are situated in isolated sites and are connected to the host by HBs O−H···O, O−H···O^-, and N^+−H···O (O3−H3A···O9, 1.877 Å, 2.717 Å, 156.1°; O9−H9B···$O5^-$, 2.049 Å, 2.874 Å, 172.0°; $N2^+$−H2B··· O9, 2.237 Å, 3.021 Å, 149.8°; O9−H9A···$O5^-$, 2.064 Å, 2.899 Å, 177.9°) (Figure 2).

The crystals of form β, which have a distinct block morphology, are of $P2_12_12_1$ symmetry and contain one zanamivir zwitterion and two water molecules in the asymmetric unit. The two water molecules, interconnected through O−H···O HB (O8−H8A···O9, 1.889 Å, 2.766 Å, 168.0°), are situated in the same isolated sites in the crystal lattice. One of the water molecules is connected to zanamivir by O−H···O and N^+−H···O HBs (O2−H2A···O8, 2.051 Å, 2.766 Å, 141.4°; O8−H8B···O4, 2.044 Å, 2.848 Å, 169.4°; $N3^+$−H3B···O8, 2.327 Å, 2.975 Å, 131.5°), whereas the other water molecule forms only an O−H··· N^+ HB (O9−H9A···$N3^+$, 2.566 Å, 3.228 Å, 136.8°) to the host (Figure 3). A detailed crystal structure analysis of both structures is presented in the Supporting Information (Figures S2 and S3).

In form α, one of the water molecules is situated in a channel and the other is in an isolated site in the crystal lattice. Water molecules situated in the isolated sites form tighter HBs relative to water molecules in the channels.[23] On the other hand, the two symmetry-independent water molecules in form β are situated in isolated sites and are hydrogen-bonded to each other as well as to zanamivir.

The difference in the molecular environment of the water molecules in the two polymorphs is generally in line with the results from the thermal analysis performed by differential scanning calorimetry (DSC) and thermogravimetric analysis (TGA). Between 25 and 110 °C, both forms undergo a weight loss of ∼10%, corresponding to desolvation by desorption of the two water molecules. The desolvation of form α proceeds in two steps corresponding to sequential removal of the water molecules, whereas form β is dehydrated in a single step. In accordance with the crystal structures, the higher dehydration temperature of form β indicates that the solvent is held more firmly in the lattice relative to form α. The anhydrous residues of forms α and β are stable up to 250 °C and decompose afterward (see the inset in Figure S4, Supporting Information). Form β shows a broad endothermic hump centered at 110 °C and does not undergo any additional thermal exchange. The single endotherm is due to the presence of two water molecules in a similar molecular environment in the crystal lattice. On the contrary, form α undergoes three sharp consecutive processes over the temperature range of 100−180 °C. The first and the second endotherms correspond to the release of water molecules from the channel and from the isolated site, the latter being coincident with the dehydration pattern observed with the β form. The third endotherm is probably due to a phase change associated with the anhydrous material.

The availability of the two crystal structures of zanamivir dihydrate and oseltamivir phosphate provides the basis for in-depth structural comparative analysis of the structures in light of the binding preferences of the inhibitor. Comparison of all available influenza neuraminidase (NA) crystal structures in complex with zanamivir or oseltamivir reveals a highly conserved inhibitor-binding pocket that is lined up with charged residues to promote tight binding interactions with the inhibitor. The interactions between oseltamivir and NA's active site residues are identical to those observed in the zanamivir complex based on amino acid sequence alignment and 3D structural comparison (Figure 4).

The carboxyl group at the C1/C2-position of oseltamivir and zanamivir, respectively, forms ionic interactions with the arginine triplet (Arg118, Arg292, and Arg371). Additional ionic interactions are observed between Glu119 and Asp151 and the primary nitrogen of zanamivir in the C4-pocket. The carbonyl oxygen of the *N*-acetyl side chain at the C5-pocket of both inhibitors forms HB interactions with Arg152. On the contrary, zanamivir, a transition-state analogue inhibitor of NA with a structure similar to sialic acid, has a higher number of binding interactions with the active site residues of NA than those observed in the oseltamivir−neuraminidase complex (Figure 4A). The guanidine side chain of zanamivir at the C4-pocket extends into the active site of NA for additional ionic interactions with Glu227. The glycerol side chain at the C6 position of zanamivir forms HBs with Arg224 and Glu276 (Figure 4A). The oxygen at position 1 of the pyran ring of zanamivir interacts with Glu277, Arg292, and Tyr406. As a result, the increased number of NA's active site interactions with zanamivir in comparison to oseltamivir can explain the reported increased clinical effectiveness of zanamivir in contrast to oseltamivir.[1,2]

In summary, with the first structure determination of two forms of zanamivir dihydrate, the most potent neuraminidase inhibitor, we demonstrated a new strategy to resolve pharmaceutical forms. Although creeping of crystallizing solutions is normally perceived as a nuisance that leads to loss of material, this example shows that, by combination with antisolvent vapor diffusion into saturated solutions, this phenomenon could be turned into an asset. The use of saturated solutions required for this method does not bring an increased cost in the procedure, because the crystallization solutions can be recycled by addition of material to the spent crystallization solution. The procedures for dissolution and crystallization of zanamivir described here are performed at room temperature, which alleviates the overall cost of the crystallization.

■ ASSOCIATED CONTENT

Supporting Information

Experimental details, X-ray crystallography, crystal structure analysis, thermal analysis, and CIF files. This material is available free of charge via the Internet at http://pubs.acs.org.

■ AUTHOR INFORMATION

Corresponding Author

*E-mail: pance.naumov@nyu.edu. Fax: (+)971-(0)2-628-8616.

Funding

This study was funded by New York University Abu Dhabi.

Notes

The authors declare no competing financial interest.

■ ACKNOWLEDGMENTS

The synchrotron radiation experiments were performed at the BL02B1 beamline of SPring-8 with the approval of the Japan Synchrotron Radiation Research Institute (JASRI) (Proposal No. 2012B1109).

■ REFERENCES

(1) Cox, N. J.; Subbarao, K. *Lancet* **1999**, *354*, 1277.
(2) Hall, C. B. *Clin. Infect. Dis.* **2007**, *45*, 353.

(3) Dawood, F. S.; Jain, S.; Finelli, L.; Shaw, M. W.; Lindstrom, S.; Garten, R. J.; Gubareva, L. V.; Xu, X.; Bridges, C. B.; Uyeki, T. M. *New Engl. J. Med.* **2009**, *360*, 2605.
(4) Oxford, J. S. *IDrugs* **2000**, *3*, 447.
(5) Air, G. M.; Ghate, A. A.; Stray, S. J. *Adv. Virus Res.* **1999**, *54*, 375.
(6) Gubareva, L. V.; Kaiser, L.; Hayden, F. G. *Lancet* **2000**, *355*, 827.
(7) Hsu, J.; Santesso, N.; Mustafa, R.; Brozek, J.; Chen, Y. L.; Hopkins, J. P.; Cheung, A.; Hovhannisyan, G.; Ivanova, L.; Flottorp, S. A.; Saeterdal, I.; Wong, A. D.; Tian, J.; Uyeki, T. M.; Akl, E. A.; Alonso-Coello, P.; Smaill, F.; Schünemann, H. J. *Ann. Intern. Med.* **2012**, *156*, 512.
(8) Hayden, F. G.; Osterhaus, A. D. M. E.; Treanor, J. J.; Fleming, D. M.; Aoki, F. Y.; Nicholson, K. G.; Bohnen, A. M.; Hirst, H. M.; Keene, O.; Wightman, K. *New Engl. J. Med.* **1997**, *337*, 874.
(9) Monto, A. S.; Fleming, D. M.; Henry, D.; de Groot, R.; Makela, M.; Klein, T.; Elliott, M.; Keene, O. N.; Man, C. Y. *J. Infect. Dis.* **1999**, *180*, 254.
(10) Elliott, M. *Philos. Trans. R. Soc. London, Ser. B.* **2001**, *356*, 1885.
(11) Chen, L. F.; Dailey, N. J.; Rao, A. K.; Fleischauer, A. T.; Greenwald, I.; Deyde, V. M.; Moore, Z. S.; Anderson, D. J.; Duffy, J.; Gubareva, L. V.; Sexton, D. J.; Fry, A. M.; Srinivasan, A.; Wolfe, C. R. *J. Infect. Dis.* **2011**, *203*, 838.
(12) Le, Q. M.; Wertheim, H. F.; Tran, N. D.; van Doorn, H. R.; Nguyen, T. H.; Horby, P. *New Engl. J. Med.* **2010**, *362*, 86.
(13) Hurt, A. C.; Hardie, K.; Wilson, N. J.; Deng, Y. M.; Osbourn, M.; Gehrig, N.; Kelso, A. *New Engl. J. Med.* **2011**, *365*, 2541.
(14) Hurt, A. C.; Hardie, K.; Wilson, N. J.; Deng, Y. M.; Osbourn, M.; Leang, S. K.; Lee, R. T.; Iannello, P.; Gehrig, N.; Shaw, R.; Wark, P.; Caldwell, N.; Givney, R. C.; Xue, L.; Maurer-Stroh, S.; Dwyer, D. E.; Wang, B.; Smith, D. W.; Levy, A.; Booy, R.; Dixit, R.; Merritt, T.; Kelso, A.; Dalton, C.; Durrheim, D.; Barr, I. G. *J. Infect. Dis.* **2012**, *206*, 148.
(15) Kidd, I. M.; Down, J.; Nastouli, E.; Shulman, R.; Grant, P. R.; Howell, D. C.; Singer, M. *Lancet* **2009**, *374*, 1036.
(16) Dulek, D. E.; Williams, J. V.; Creech, C. B.; Schulert, A. K.; Frangoul, H. A.; Domm, J.; Denison, M. R.; Chappell, J. D. *Clin. Infect. Dis.* **2010**, *50*, 1493.
(17) Gaur, A. H.; Bagga, B.; Barman, S.; Hayden, R.; Lamptey, A.; Hoffman, J. M.; Bhojwani, D.; Flynn, P. M.; Tuomanen, E.; Webby, R. *New Engl. J. Med.* **2010**, *362*, 88.
(18) Härter, G.; Zimmermann, O.; Maier, L.; Schubert, A.; Mertens, T.; Kern, P.; Wöhrle, J. *Clin. Infect. Dis.* **2010**, *50*, 1249.
(19) Chan-Tack, K. M.; Gao, A.; Himaya, A. C.; Thompson, E. G.; Singer, M. E.; Uyeki, T. M.; Birnkrant, D. B. *J. Infect. Dis.* **2013**, *207*, 196.
(20) Moscona, A. *New Engl. J. Med.* **2005**, *353*, 2633.
(21) Naumov, P.; Yasuda, N.; Rabeh, W. M.; Bernstein, J. *Chem. Commun.* **2013**, *49*, 1948.
(22) van Enckevort, W. J. P.; Los, J. H. *Cryst. Growth Des.* **2013**, *13*, 1838.
(23) Fucke, K.; Steed, J. W. *Water* **2010**, *2*, 333.